

Evaluation of a gamma camera system for the RITS-6 accelerator using the self-magnetic pinch diode

Timothy J. Webb^{*a}, Mark L. Kiefer^a, Raymond Gignac^b, Stuart A. Baker^b

^a Sandia National Laboratories, Albuquerque, NM 87185

^bNational Security Technologies, LLC, Las Vegas, NV 89193

ABSTRACT

The self-magnetic pinch (SMP) diode¹ is an intense radiographic source fielded on the Radiographic Integrated Test Stand (RITS-6) accelerator at Sandia National Laboratories in Albuquerque, NM. The accelerator is an inductive voltage adder (IVA) that can operate from 2-10 MV with currents up to 160 kA (at 7 MV). The SMP diode consists of an annular cathode separated from a flat anode, holding the bremsstrahlung conversion target, by a vacuum gap. Until recently the primary imaging diagnostic utilized image plates (storage phosphors) which has generally low DQE at these photon energies along with other problems. The benefits of using image plates include a high-dynamic range, good spatial resolution, and ease of use. A scintillator-based X-ray imaging system or “gamma camera” has been fielded in front of RITS and the SMP diode which has been able to provide vastly superior images in terms of signal-to-noise with similar resolution and acceptable dynamic range.

Keywords: Flash x-ray radiography, scintillators, computed radiography, gamma camera

1. INTRODUCTION

The self-magnetic pinch (SMP) diode¹ is being developed at Sandia National Laboratories on the RITS-6 accelerator for flash x-radiography. The key parameters for these sources include, but are not limited to, dose, spot size, x-ray spectrum, and pulse width. Details of these parameters for the SMP will be given below. A radiographic system includes many other components including shielding, conjugate distances, and especially the imaging system. Typically most of the investment of the radiographic system focuses on the x-ray source where initially the cheapest available imaging system is used to evaluate the source performance. However significant increases in the quality of the resulting radiographs can result in even modest improvements in the detector system. When RITS-6 was first being brought up, x-ray film was first used. Later image plates were, and still are, utilized for their high resolution and sensitivity but may have relatively high noise in some situations. A gamma camera system has been developed and fielded in front of RITS-6 and the SMP diode which results in much higher signal-to-noise characteristics which is more suitable for real radiographic experiments.

2. OPERATION AND PERFORMANCE OF THE SMP DIODE

The SMP diode is a simple and low-cost method for generating a tightly-focused, intense electron beam which impinges on an x-ray converter to produce a small, bright, flash x-ray source. It is driven by a pulsed power system at high voltage. The diode configuration is shown below in Figure 1. The electron beam is produced at the tip of the small diameter hollow cathode. The cathode tip is covered with colloidal silver paint which ensures fast and uniform emission of electrons. The electrons traverse the anode-cathode (A-K) gap to the anode and focuses tightly onto the anode foil due to the beam’s self-magnetic field. The electrons then strike the ~ 1mm thick bremsstrahlung Tantalum converter plate behind the foil and produces the x-ray spot. The cathode diameter and the AK gap are adjusted depending on the voltage of the pulse power driver for optimal performance (smallest spot while retaining a stable x-ray pulse width). Much of the SMP development work involves optimizing the geometry and materials to maintain a careful balance between achieving the smallest spot possible while maintaining a high dose.

^{*}tjwebb@sandia.gov, ph: (505) 284-9865

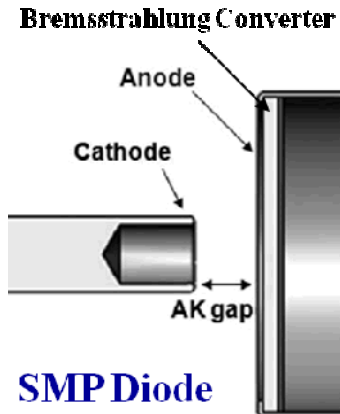


Figure 1. Diagram of the SMP diode hardware.

The doses and spot sizes of the SMP diode depend on the exact diode configuration and voltage. At about 7 MV which represents the approximately nominal configuration of the SMP at RITS-6 the dose is about 300-350 rads @ 1 m. The spot sizes can be characterized in a number of ways in direct analogy to the blur function often applied in optics such as the edge-spread function (ESF), line-spread function (LSF), and point-spread function (PSF). A simple spot size metric can be associated with each of these profiles such as the FWHM of the LSF or PSF or the width of the ESF. The width of the ESF is typically < 3 mm while the FWHM of the LSF or PSF is less than 2 mm.

The x-ray spectrum is difficult to measure directly. However for radiographic purposes the aspect of the x-ray spectrum that is pertinent is the relation of x-ray transmission through a given material thickness (which can be a function of atomic number) known as the transmission curve. The transmission curve is part of the process of calibrating a radiograph to go from transmission to areal density.



Figure 2. Photo of the RITS-6 accelerator. The diode is at the end of the accelerator towards the upper-right behind a shield wall.

3. RADIOGRAPHIC INTEGRATED TEST STAND (RITS-6)

RITS-6² is an inductive voltage adder (IVA) accelerator designed to drive a variety of electron beam diodes, usually in negative polarity from \sim 3 MV to above 10 MV. A photo of RITS-6 is shown in Figure 2. There is a succession of pulse compression stages going from a single Marx generator which discharges into two intermediate storage capacitors which each feed three pulse-forming lines (PFL) through a laser-triggered gas switch. Six accelerating cells are powered by one of the PFLs through a single feed. The voltage pulse is then applied to a vacuum transmission line. The voltage on the transmission line center conductor is high enough to result in electron emission, but the current is high enough to result in magnetic insulation the result being a magnetically insulated transmission line (MITL). The diode load, such as the SMP diode reported on here, resides at the end of the MITL.

4. DETECTOR SYSTEM CHARACTERIZATION

Fuji image plates (IPs) have been used regularly in front of RITS-6 for about the last decade. The use of image plates, also known as storage phosphors, constitutes what is known as Computed Radiography (CR). The benefits of IPs include ease-of-use, high-dynamic range, high-sensitivity (below 1 mrad), and high sensitivity. The construction and general properties of the IP are included in many other references³⁻⁴. The chief downsides of using IPs in our application of high-energy x-rays are the relatively low x-ray absorption efficiency of the image plates and the difficulties of removing fixed-pattern noise (FPN) from the images. The low efficiency results from the relatively thin active layer of the plates (few hundred microns at most) and the fact that the readout process only removes a fraction of the stored energy in the phosphor. This combines to result in quite low detective quantum efficiencies of a few tenths of a percent at our MeV photon energies. The FPN results from scanner non-uniformities and imperfections in the each image plate. It is difficult to fully remove FPN using flat-fielding techniques from the images because the flatfield and the image to be flat-fielded must be properly spatially registered. The fielding and scanning of the image plates each include some spatial ambiguity beyond the pixel-size scale required for effective FPN removal.

The IPs once exposed to x-rays must be shielded from room light and are thus enclosed in a cassette. The IPs are sandwiched between two layers of 0.4 mm-thick Ta plates which increase the IPs signal contributions from high-energy x-rays and reduces the sensitivity to low-energy x-rays which forms a larger component of the background “scatter” which reduces image contrast. There are two types of Fuji image plates typically employed at RITS, MS (white colored) and SR (blur colored). The MS type has a factor 2-3 times higher signal than SR. The SR plate is designed to have higher resolution due to less blur in the scanning process, however the overall resolution in the RITS beam does not seem to be significantly different between the two types which suggest that the resolution is not dominated by the scanner blur. Various combinations of scanner sensitivities and IP types allow the image plates to read well below 1 mrad to above 10 rads. Multiple image plates may be stacked and averaged, but the difficulties of image registration and the dominance of FPN at high signal levels limit the effectiveness of stacked plates to increasing the signal-to-noise ratio (SNR).

A “gamma camera” system has had a number of iterations in the history of RITS. A gamma camera consists, in general, of a coupled scintillator (usually an inorganic), mirror, lens, and CCD. Various typical scintillators include BGO, CsI, NaI, and most commonly LSO or LYSO which is used in the latest incarnation of the gamma camera. A diagram of the gamma camera is shown in Figure 3. The system is enclosed in a screen box to shield the CCD electronics from the EMP when RITS-6 fires. The primary x-ray beam illuminates the scintillator which converts some of the energy to blue light, producing the image which is, in turn, collected by the lens and CCD. The 45° pellicle mirror is used to get the lens and CCD out of the path of the primary x-ray beam. The thickness of LYSO scintillator of the data presented here is 10 mm though 2.7 mm and 5 mm thicknesses are available.

This system is a single-shot design primarily limited by the current CCD chip which can only read a single-image at a time. The time-response is also limited by the LYSO which has a \sim 40 ns decay time which means that resolving images within the radiation pulse is not possible. However, as an aside, if multiple x-ray pulses come at $>$ 100 ns intervals, then this system can generate multiple images with a multi-frame CCD or with multiple, gated, lens-CCD systems viewing the scintillator, but this is not relevant for RITS since it is a single-shot machine.

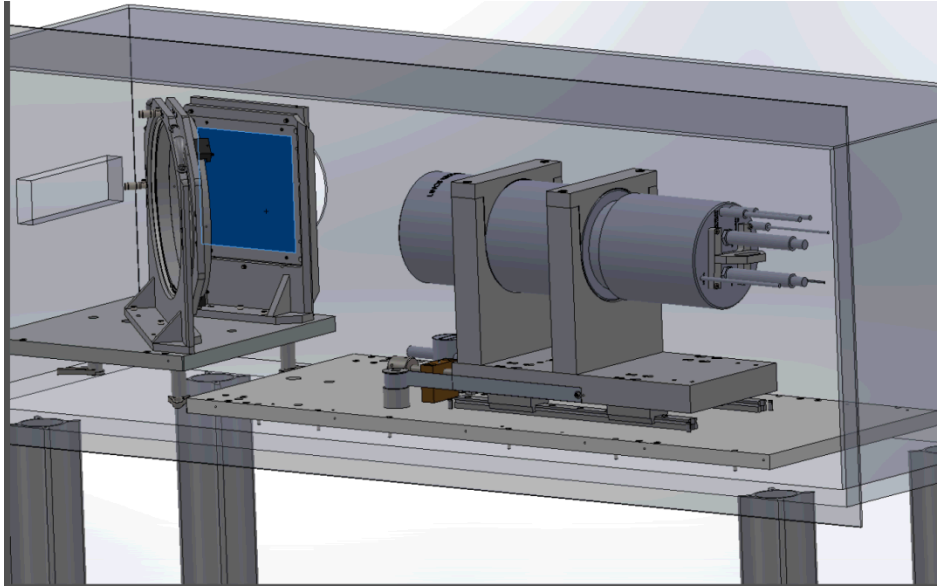


Figure 3. Diagram of the gamma camera. The 200 mm x 200 mm LYSO scintillator is the blue square on the left.

Several scientific-grade CCDs have been used over the course of time, all very similar, but primarily varying in format. They are Spectral Instruments 1100 Series cameras. The back-thinned sensors are either 25 μm 2000 x 2000 pixels, or 15 μm 4000 x 4000 pixels though the 4K cameras are hardware binned 2x2. They have been designed to mount to the LINOS lens, and a vacuum is applied (< 10 mTorr) on the CCD chip with the back of the lens acting as one of the vacuum seals. These cameras use thermo-electric coolers, and the cameras are cooled to -60° C to -65° C.

The overall detector blur is characterized using a 10-cm thick Tungsten edge (called a “rolled edge”) in near-contact to the scintillator to measure the ESF from which the LSF and so on can be calculated. An example image of the rolled edge is shown in Figure 4. The ESF is taken across a horizontal line-out, averaged over many vertical pixels, near the center of the image. The tilt in the rolled edge does, in principle, allow sub-pixel sampling of the ESF, but it turns out that the liming resolution is well below the Nyquist frequency. The pixel size at the scintillator plane varies with the camera but is less than 0.1 mm.

The LSF of the gamma camera is shown in Figure 5. There were two F-numbers tested here, F/2 and F/8 (note: these are CCD-side F-numbers). The scintillator thickness is 1 cm. The depth-of-field of the lens at F/2 is somewhat less than the scintillator thickness, but the entire scintillator is within the depth-of-field at F/8 but at reduced light output. It has been observed that to image through relatively thick objects, F/2 is required. Conversely the image saturates in the “free field” (no object) at F/2, but F/8 is in an acceptable range of the CCD sensitivity. There is obviously less blur using F/8 though whether this is entirely due to depth-of-field effects still must be evaluated. It also may be the case that the lens itself may have less blur at F/8. Nevertheless it is clear that both scintillator and optical effects must be included in the total blur.

The gamma camera MTF using the two settings of the lens of the gamma and the image plate is shown in Figure 6. There is a similar message in comparing the two F-number results as explained above. There is an interesting difference at low frequency between the gamma camera and image plates. The image plates seem to have better contrast at low frequency. There is strong evidence that the gamma camera is susceptible to additional long-range blurring due to optical light scatter within the monolithic scintillator. This is referred to sometimes as “tile glow.” It is likely a function of the scintillator thickness and the size of the scintillator tile. The gamma camera scintillator shown here has three scintillator tiles with the boundaries between them blackened to prevent light cross-over. Image plates do not have intrinsic tile glow effects, but there is an observed low-level, long range blur in one direction due to an optical waveguide employed in the scanner but apparently not as pronounced as the scintillator tile glow.

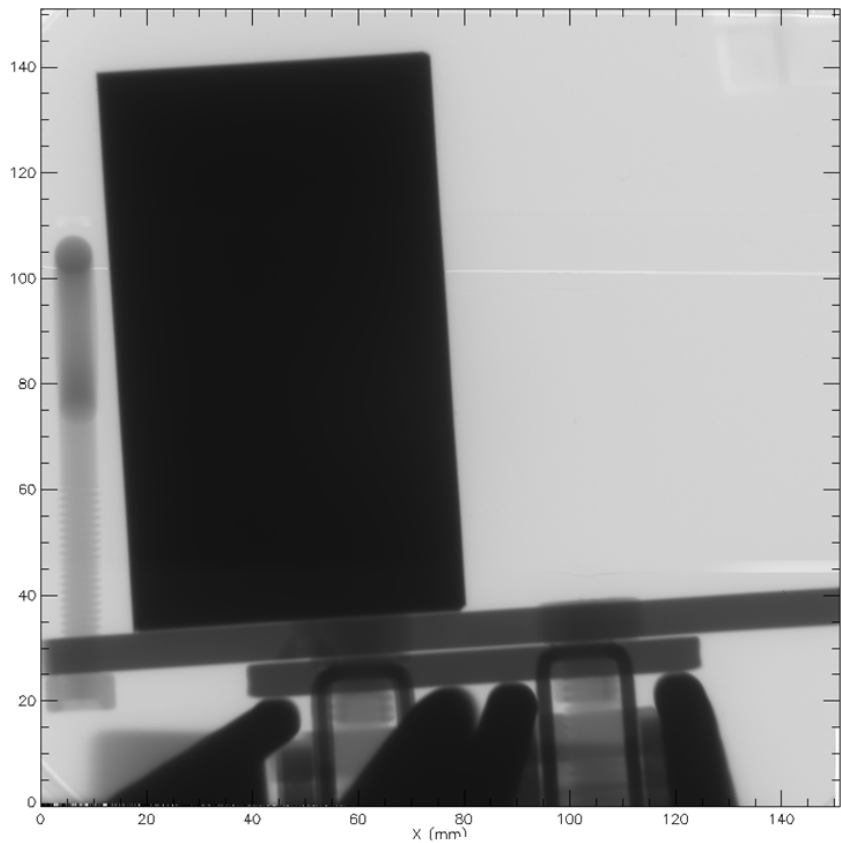


Figure 4. Radiograph of the “rolled edge” in near contact with the scintillator to measure the ESF.

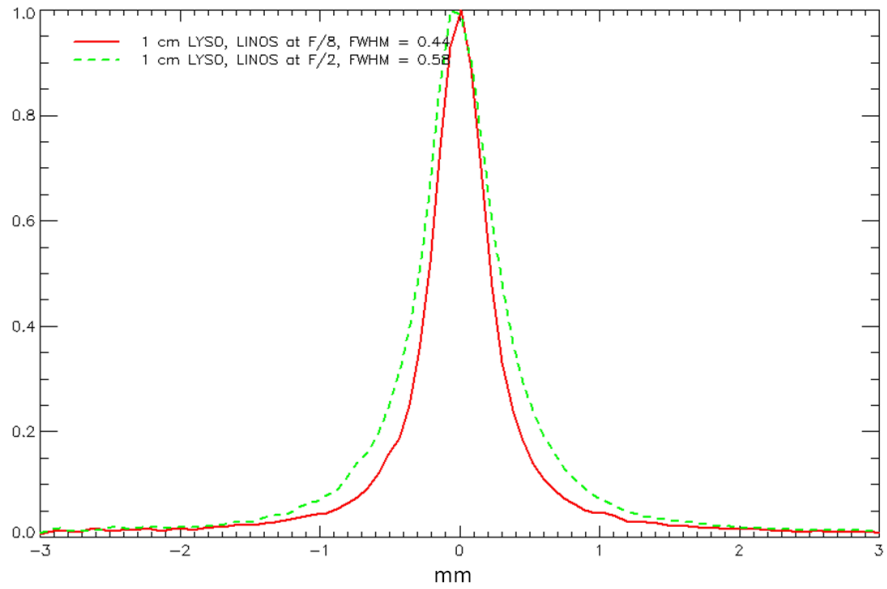


Figure 5. Line-spread function of the gamma camera system measured from data similar to Figure 4.

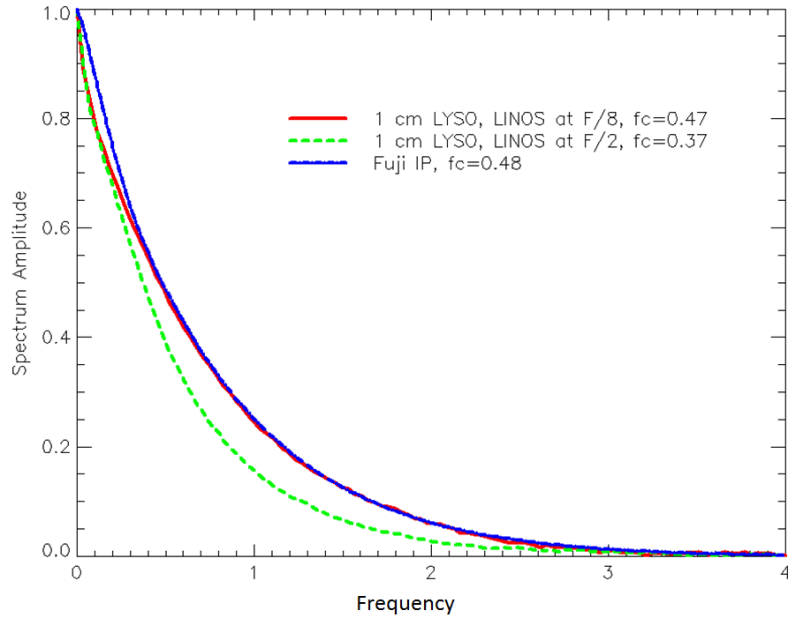


Figure 6. Modulation Transfer Functions (MTF) of the gamma camera (two F-numbers) and the image plates.

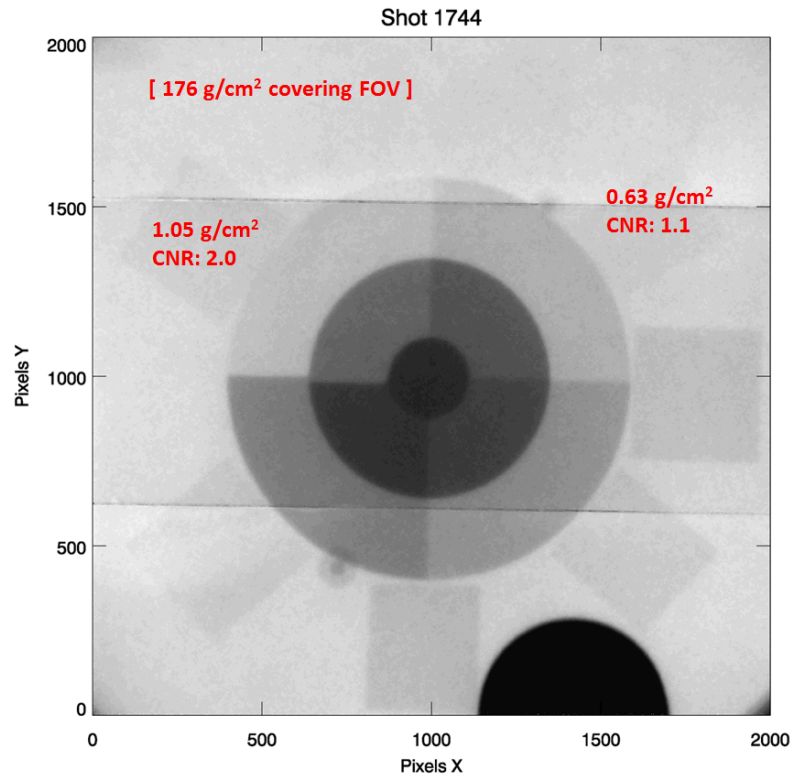


Figure 7. Radiograph of a step wedge using the gamma camera. The areal density resolution is given by the smallest step where the CNR > 1 . There are thinner steps around the perimeter of the circular step wedge that cannot be resolved at this noise level.

5. STEP WEDGE DEMONSTRATION

A step wedge is a radiographic test object used to measure the transmission curves of the x-ray spectrum. It can also be used to evaluate the ability to measure areal density “resolution.” Changes in areal density must be larger than the local noise level in order to be resolved. This may be quantified by the contrast-to-noise ratio (CNR) for a particular step on the step wedge which must be greater than one in order to be considered resolved. A radiograph of a step wedge is shown in Figure 7 using the gamma camera. A uniform thickness of 176 g/cm^2 fills the field-of-view (FOV). The limiting areal density resolution is defined as the first “step” where the $\text{CNR} > 1$ which is shown in this case to be 0.63 g/cm^2 . Thicker steps are obviously more easily resolved. Future work will compare similar data to the image plate, but it has been already observed that the thinnest steps cannot be resolved on a pixel level by the image plates due to its much lower SNR.

6. CONCLUSIONS

Two imaging systems, image plates and a gamma camera are used at RITS-6 to study the characteristics of the SMP diode. Each of these detector systems has benefits and drawbacks. It has been shown that the resolution of the gamma camera system has better SNR performance and similar resolution to the image plates. Fixed-pattern noise can be removed from gamma camera images due to flatfield-correction techniques but are difficult to apply to image plates. Scintillators display tile glow which are not present on image plates (though other blur effects occur). Future work will consider optimization of the gamma camera CCD settings, scintillator material and thickness, and lens types and apertures.

ACKNOWLEDGEMENTS

The authors would like to thank the operations team of RITS-6 as well as various personal at the National Security Technology, Los Alamos Operations for their help in setting up the gamma camera and characterizing the CCD cameras. We also acknowledge the many helpful discussions of Steve Lutz (NSTec).

This work was also supported by the Sandia National Laboratories, Sandia Corporation, a wholly owned subsidiary of Lockheed Martin Company, for the U.S. Department of Energy’s National Nuclear Security Administration under Contract No. DE-AC04-94AL85000.

REFERENCES

- [1] Kahn, K. D. et al. “Overview of magnetically pinched-diode investigations on RITS-6.” *IEEE Trans. Plasma Sci.*, vol. 38, no. 10, pp. 2652-2662, Oct. 2010. Davis, A. R., Bush, C., Harvey, J. C. and Foley, M. F., “Fresnel lenses in rear projection displays,” *SID Int. Symp. Digest Tech. Papers* 32(1), 934-937 (2001).
- [2] Johnson, D. L., *et al.*, “Status of the 10 MV 120 kA RITS-6 inductive voltage adder.” *Proc. 15th IEEE Int. Pulsed Power Conf.*, Monterrey, CA, 2005, pp. 314-317.
- [3] Rowlands, J. A., “The physics of computed radiography,” *Phys. Med. Biol.* 47 (2002) R123–R166.
- [4] Meadowcroft, A. L., Bentley, C. D., and Stott, E. N., “Evaluation of the sensitivity and fading characteristics of an image plate system for x-ray diagnostics,” *Rev. Sci. Instr.* 79, 113102 2008